Absolute and global instability of mixing layers without reverse flow

R. Danyi

Department of Mathematics at Keele University

Waves in the Flows, Prague 2018

Motivation

- There is fundamental question about stability of stably stratified flows which pops out in many different context such as dynamics of oceans, atmosphere or industrial processes where mixing is of interest. We are looking at fundamental hydrodynamic problem and mechanisms of the mixing, and for application we consider near shore sea regions, where our proposed theory might be applicable.

Content

- Introduction to the problem and Taylor-Goldstein (TG) equation
- Investigation of absolute instability (AI)
- Effects of boundaries on AI
- Results and application to near shore sea
- Investigation of global instability in near shore sea

Mixing problem

- Parallel stratified shear layers without reverse flow which develop slowly in streamwise direction.
- Typical in near shore region, river plumes, estuaries, etc.

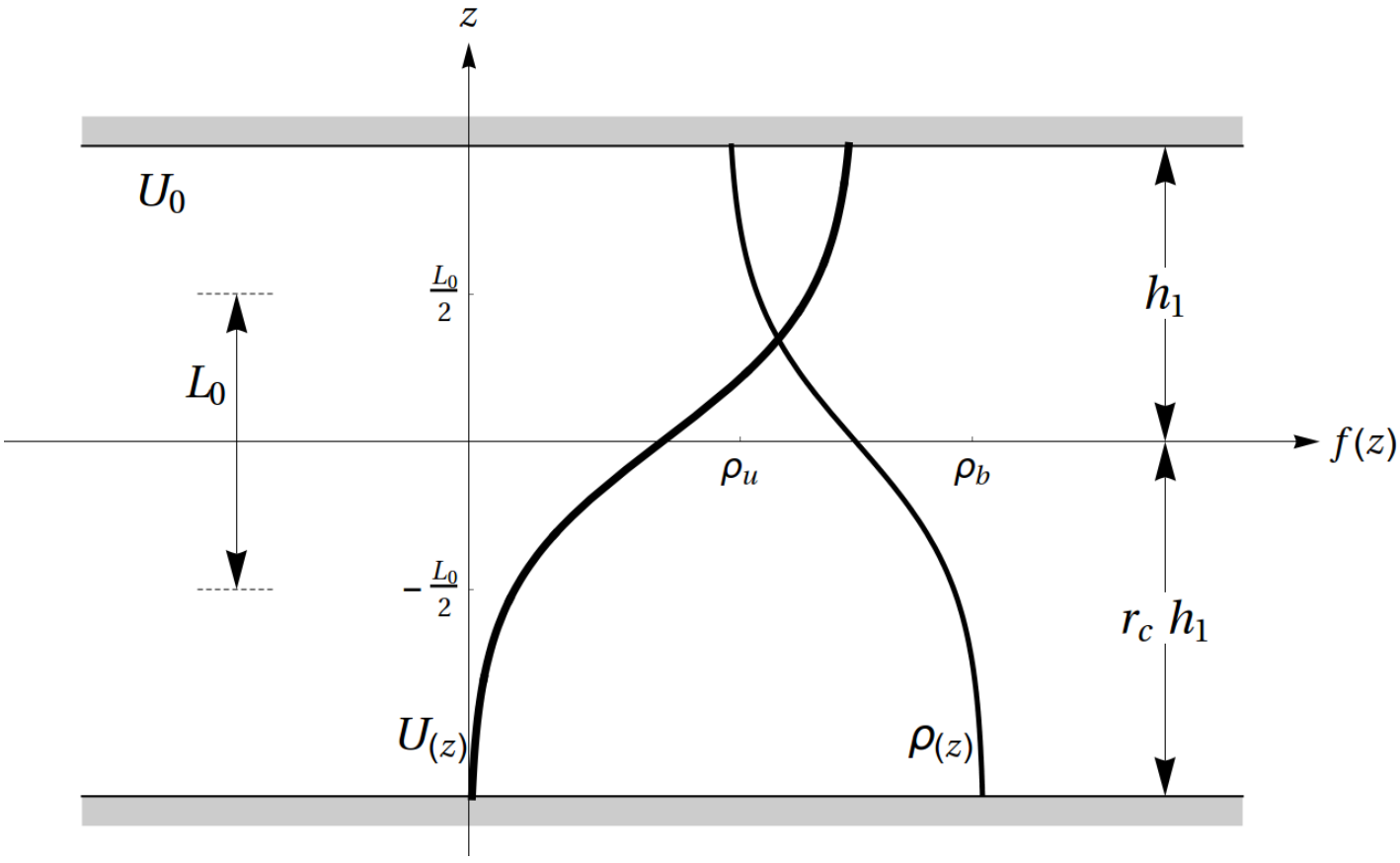

- Scaling by U_0, L_0 and ρ_{mean}.

Inviscid equation of motion

- We neglect viscosity, since we are investigating instabilities with relatively small time scale in comparison to viscous effect (large Reynolds number $U_0 L_0/\nu$).
- These flows often exhibits strong instabilities which are well described by inviscid equations.

$$\left.\begin{aligned} \rho\left(\frac{\partial \bar{u}}{\partial t} + \bar{u}\cdot\nabla\bar{u}\right) &= -\nabla p + \bar{g}\rho \\ \bar{\nabla}\cdot\bar{u} &= 0 \\ \frac{\partial \rho}{\partial t} + \bar{u}\cdot\nabla\rho &= 0 \end{aligned}\right\} \tag{1}$$

TG equation

- We impose normal mode analysis in form

$$\hat{w}e^{i\alpha(x-ct)}, \text{with resultant frequency } \omega = c\alpha. \tag{2}$$

- Equations of motion (1) can be linearised into TG equation

$$\underbrace{(U-c)\{D^2\hat{w}-\alpha^2\hat{w}\}-U''\hat{w}}_{\text{Rayleigh equation}}\underbrace{-\frac{\tilde{\rho}'}{F^2(U-c)\tilde{\rho}}\hat{w}}_{\text{Buoyancy term}}+\underbrace{\tilde{\rho}'/\tilde{\rho}\{(U-c)D\hat{w}-U'\hat{w}\}}_{\text{Inertia term}}=0 \tag{3}$$

where $F = U_0/\sqrt{gL_0}$ and boundary conditions are (rigid lid conditions)

$$\hat{w} = 0 \text{ at } z = h_1, r_c\ h_1. \tag{4}$$

- see Drazin and Reid 1981. TG equation has been studied extensively for many years, but mostly for temporal instability.

An example of temporal stability result

Let fix $\tilde{\rho} = const.$, $U(z) = (1 + Tanh[5z])/2$, $h_1 = 5$, $r_c = 2.5$

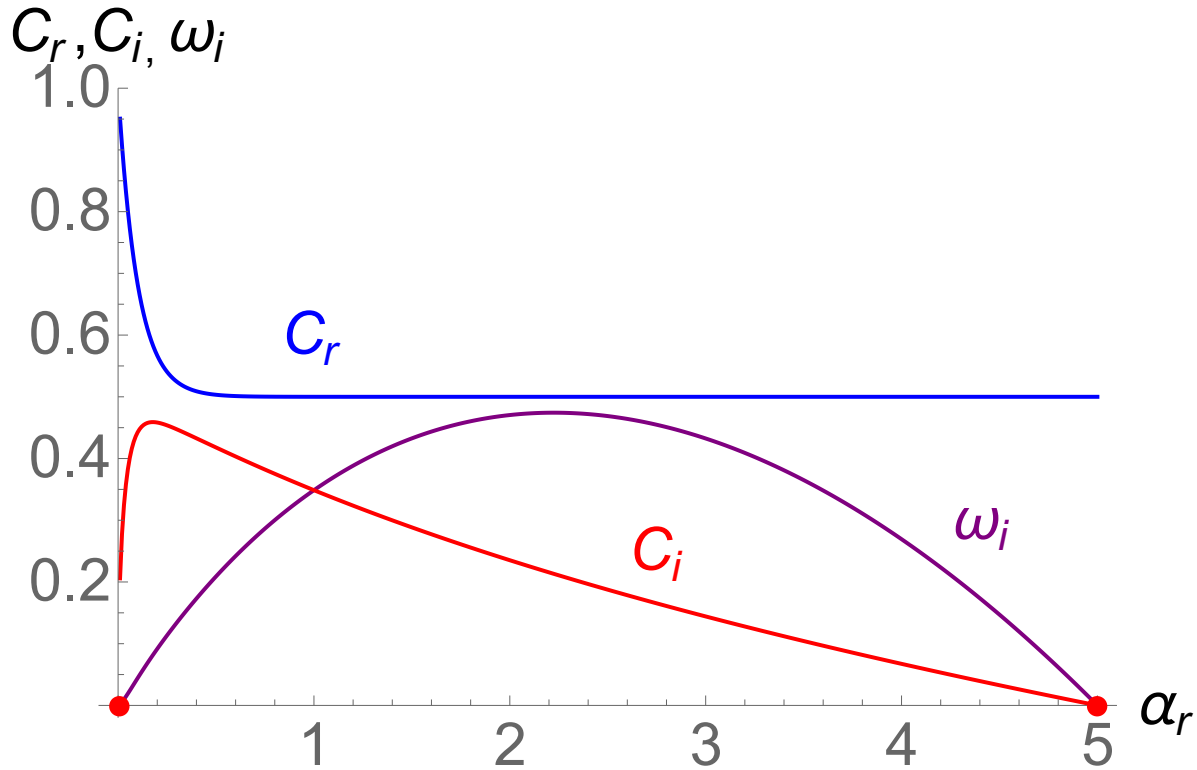

Hence max $\omega_i = 0.47$ for $\alpha_r = 2.22$ with $c_i = 0.21$ and $c_r = 0.5$.
However temporal stability analysis will not tell us how the disturbance will behave in space (as it leaves the frame of reference) and hence absolute stability analysis is needed.

Introduction to absolute instability

- Space-time diagram for growing disturbances in parallel flow.

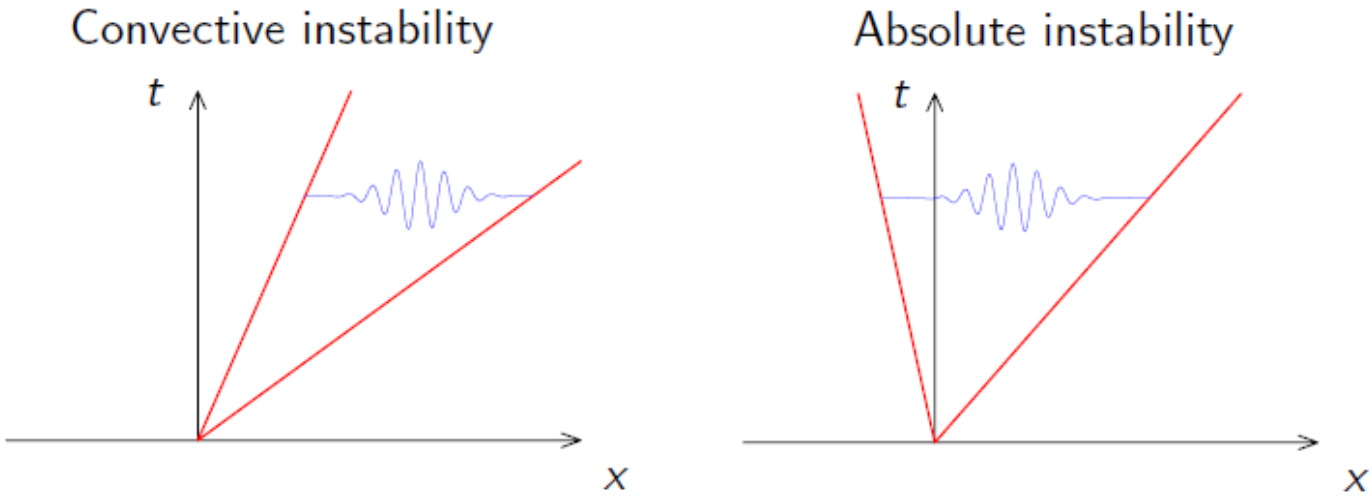

- Convective growth propagates away down stream leaving the flow undisturbed.
- Absolute growth will mix the flow and destroy the initial profiles in the frame of reference.
- We want to determine which of those we have using Briggs saddle point method (see Briggs 1964) where

$$\frac{\partial \omega}{\partial \alpha} = 0, \mathrm{Im}(\omega) > 0. \tag{5}$$

Results in complex α plane

- In the original problems people usually ignore the boundaries where possible and found that for AI the reverse flow is necessary.
- Results for unbounded homogeneous counter-flow and co-flow in complex alpha plane

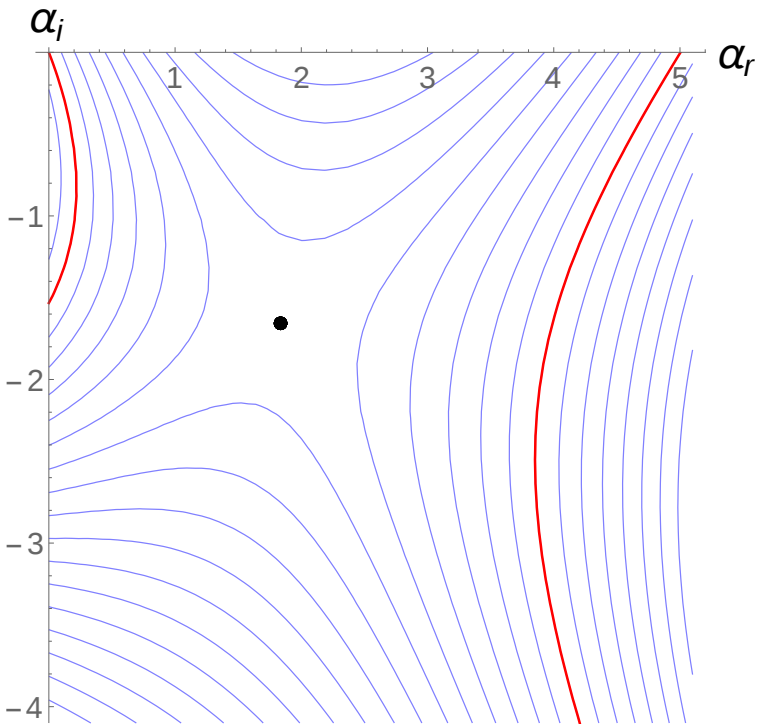

Figure: Counter-flow

Results in complex α plane

- In the original problems people usually ignore the boundaries where possible and found that for AI the reverse flow is necessary.
- Results for unbounded homogeneous counter-flow and co-flow in complex alpha plane

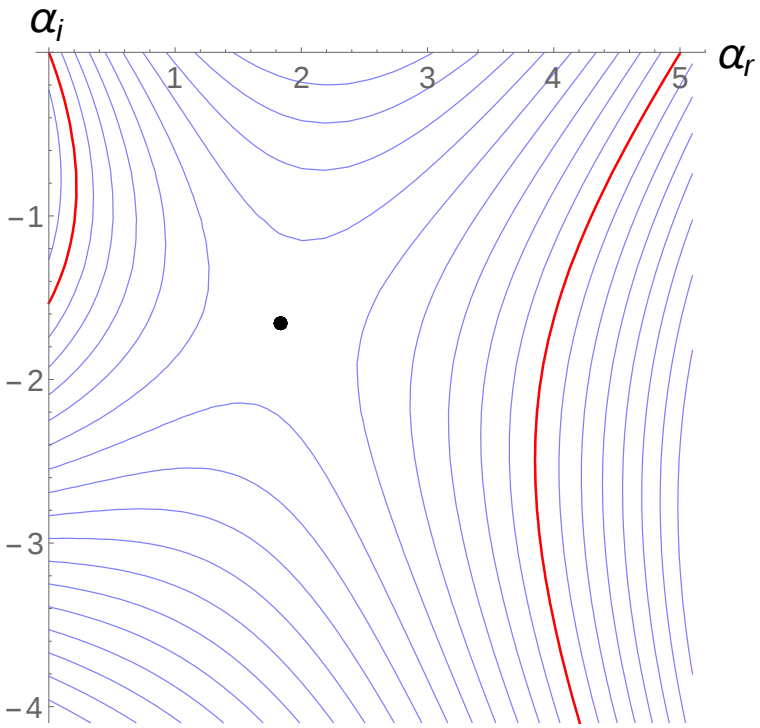

Figure: Counter-flow

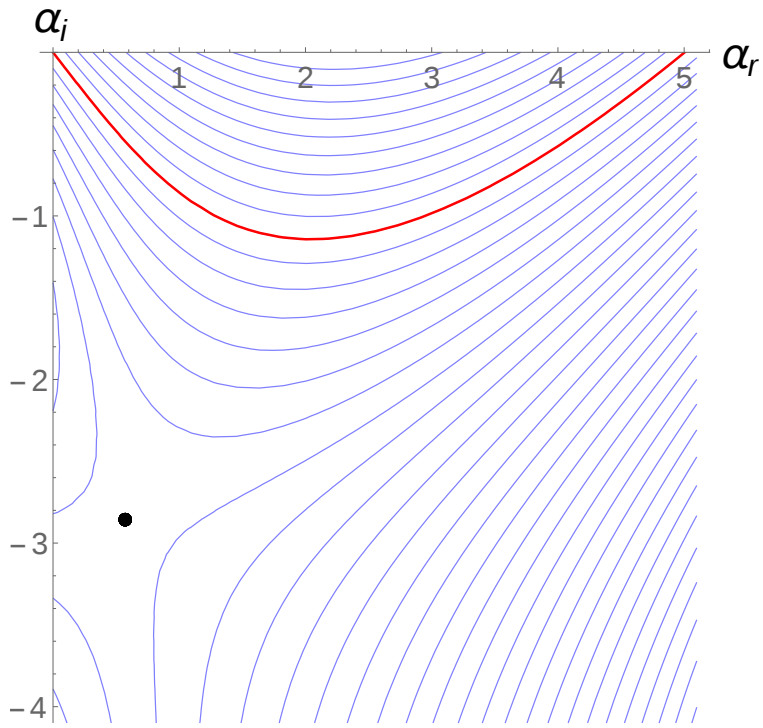

Figure: Co-flow

Effect of boundary on AI, reviewing Healey 2009

- Healey 2009 showed that boundaries placed at particular place will produce AI for flow without reverse flow. For example by adding top boundary at $h_1 = 5$ and bottom boundary at $h_2 = r_c\ h_1$, with $r_c = 2.5$.

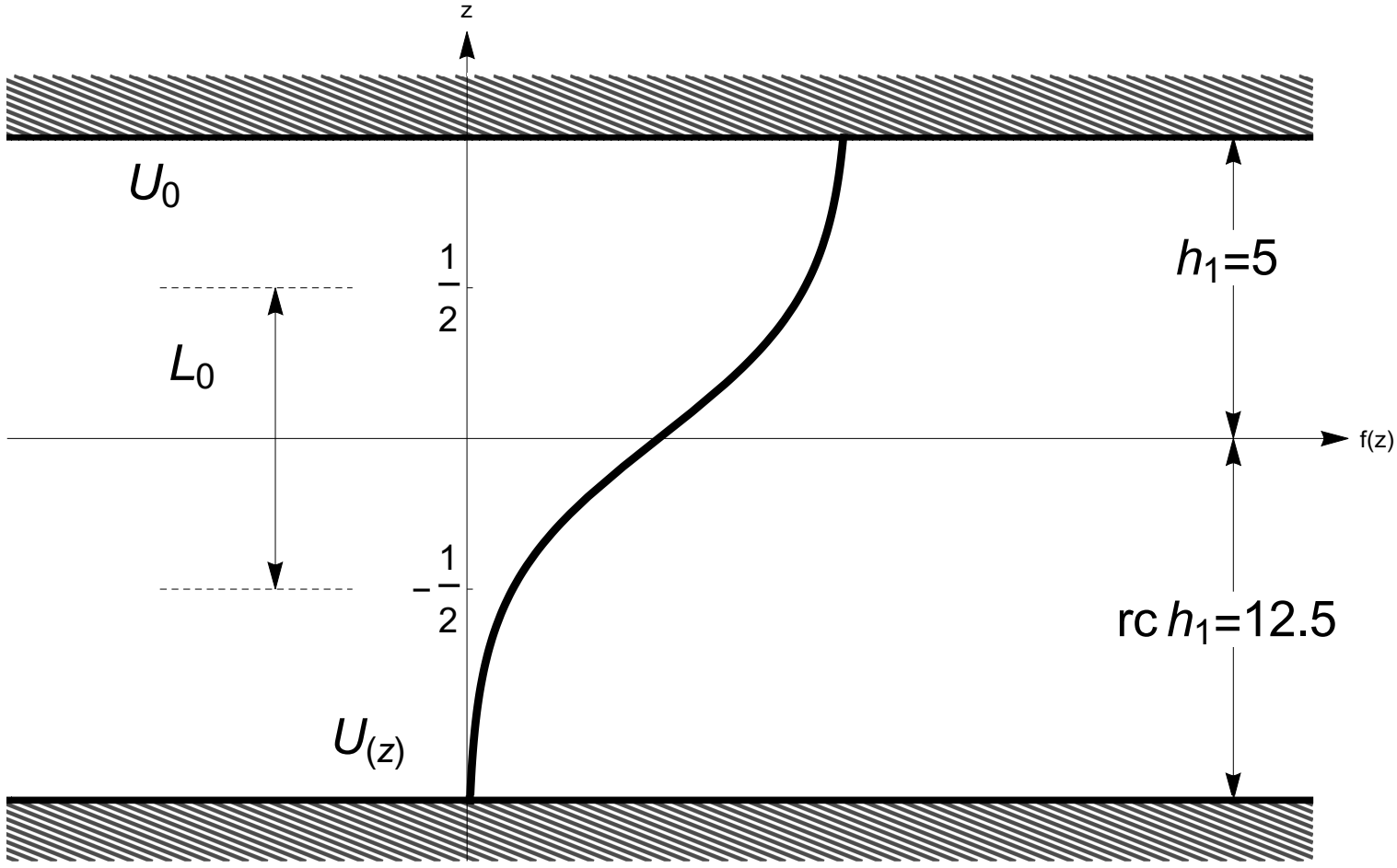

Effect of boundary on AI, reviewing Healey 2009

- Adding boundary to the problem results in poles along α_i axis,

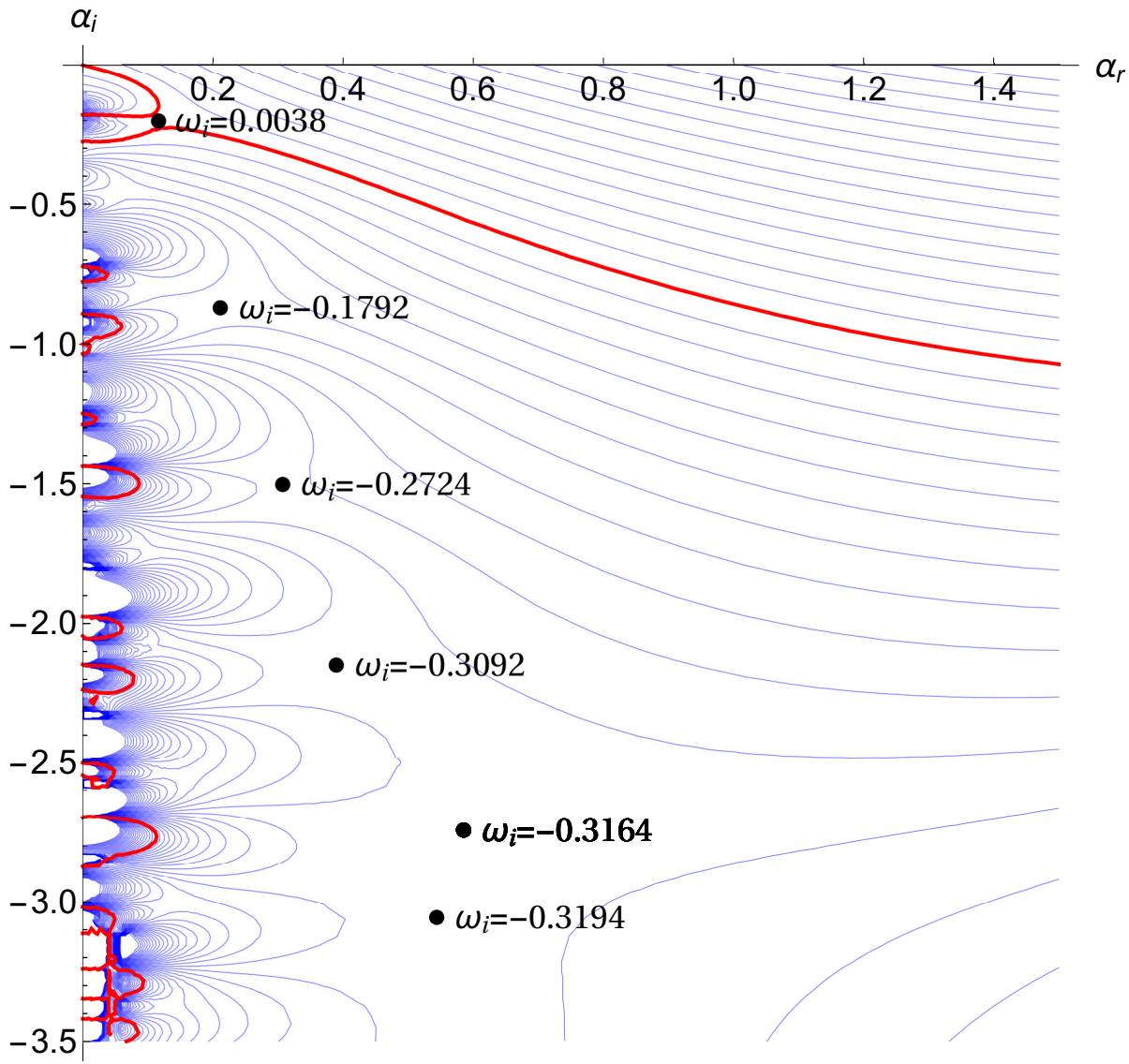

where the saddle closest to the origin has value $\omega_i = 0.0038$.

Result for homogeneous flow

- We investigate the parameter space where AI is present.

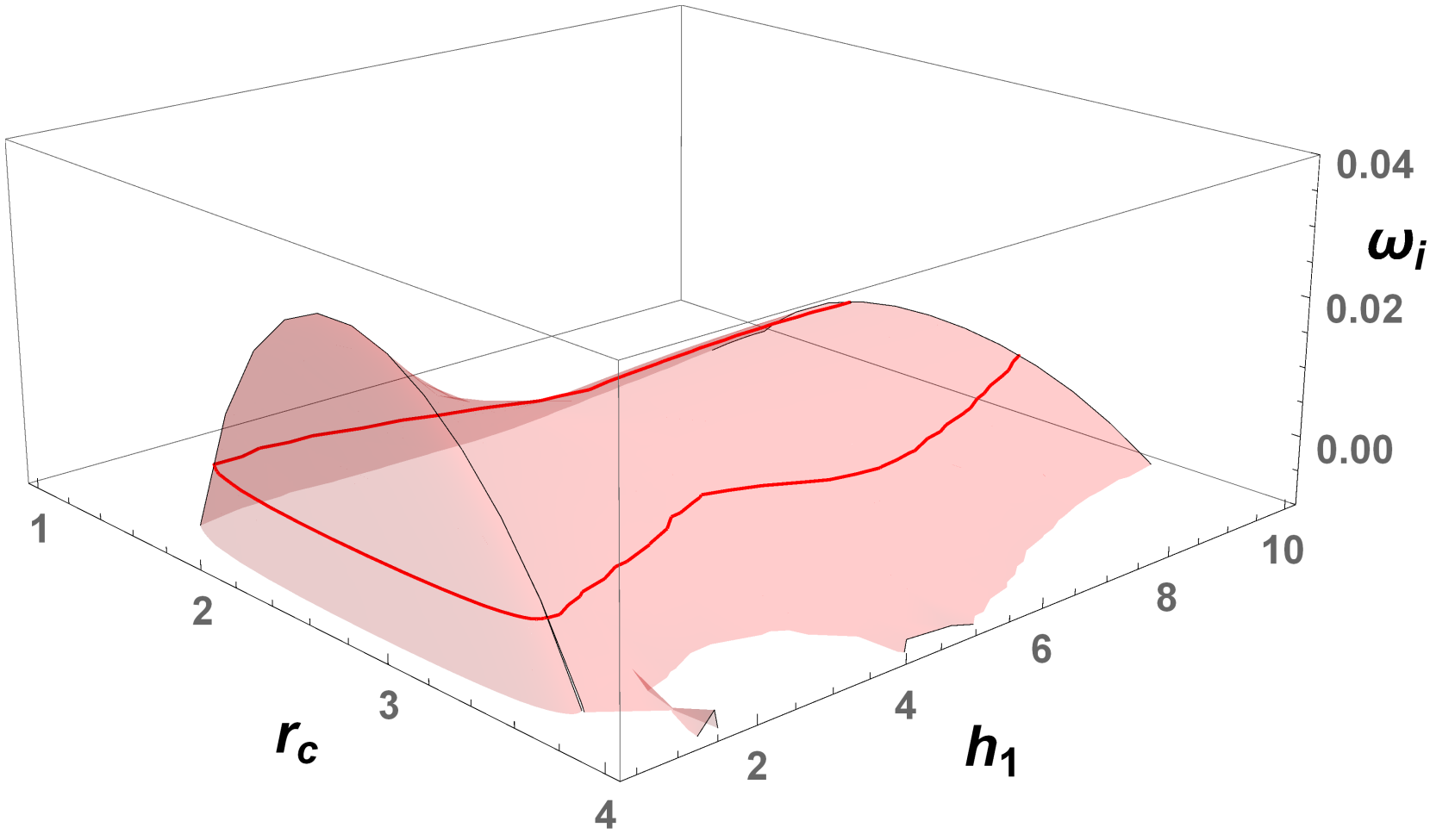

Result for stratified flow with $J_0 = 0.01$

- AI is still present for stratified flows. Define $J_0 = dgL_0/U_0^2$, where $d = (1 - \rho_{up}/\rho_{bot})/(1 + \rho_{up}/\rho_{bot})$

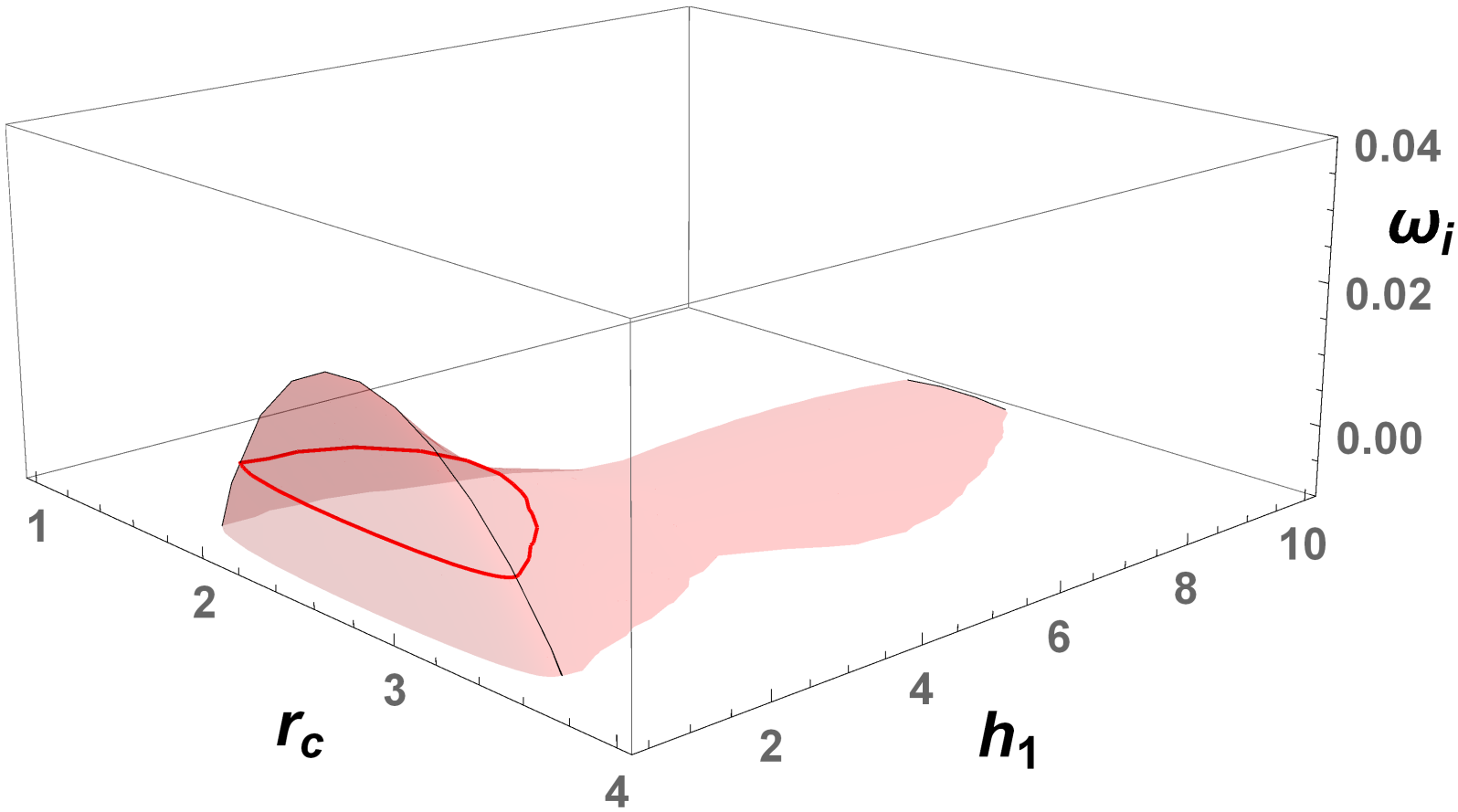

Neutral surface

- Combination of neutral curves for varying J_0 leads to neutral surface showing parameter space where AI is present. Max$J_0 \approx 0.025$ with boundaries placed at particular position $h_1 \approx 1, r_c \approx 2.5$.

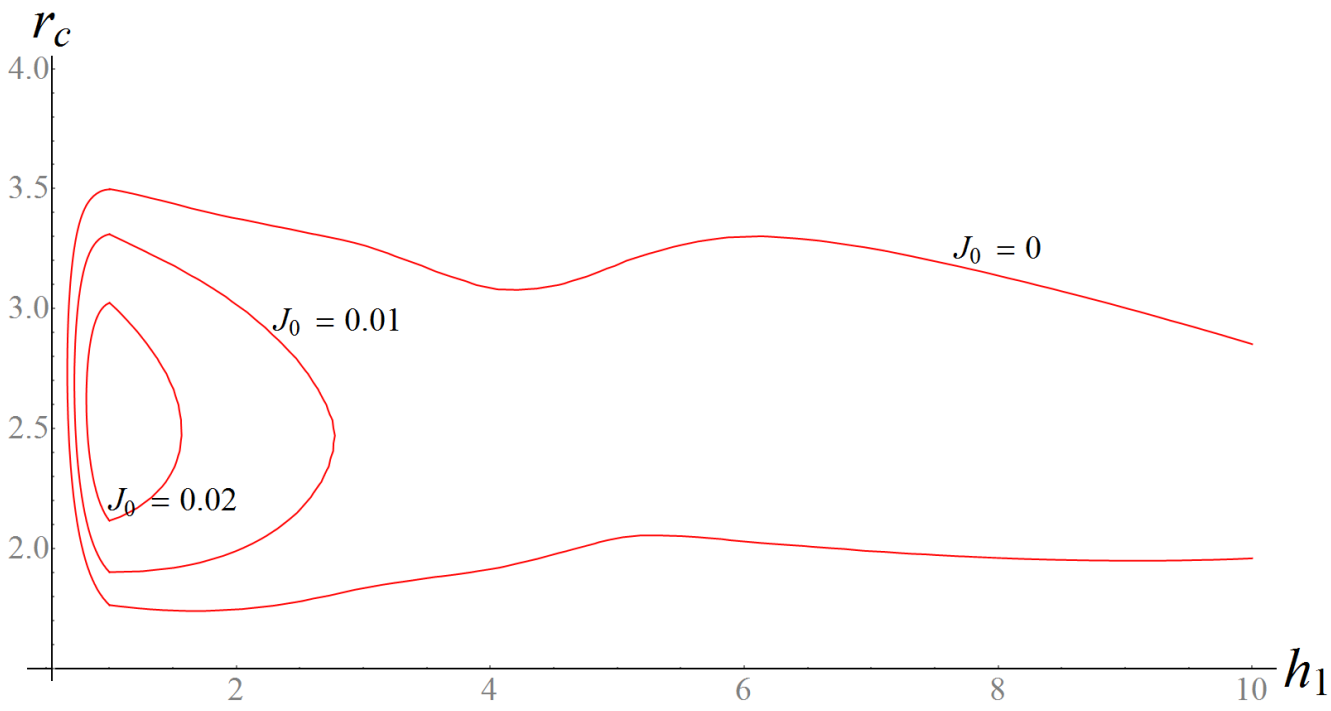

Near shore sea problem

- This means that there is possibility of AI in near shore sea region where the offshore or inshore wind will generate the required co-flow velocity profile, the temperature difference or salinity provides stratification, sea surface and sea bed are the boundaries.

Sloping bottom boundary

- Topography variation of the sea bed may result in a finite range where AI will be present. Creating zone of AI parallel to the shore.

Sloping bottom boundary

- Topography variation of the sea bed may result in a finite range where AI will be present. Creating zone of AI parallel to the shore.

Sloping bottom boundary

- Topography variation of the sea bed may result in a finite range where AI will be present. Creating zone of AI parallel to the shore.

Sloping bottom boundary

- Topography variation of the sea bed may result in a finite range where AI will be present. Creating zone of AI parallel to the shore.

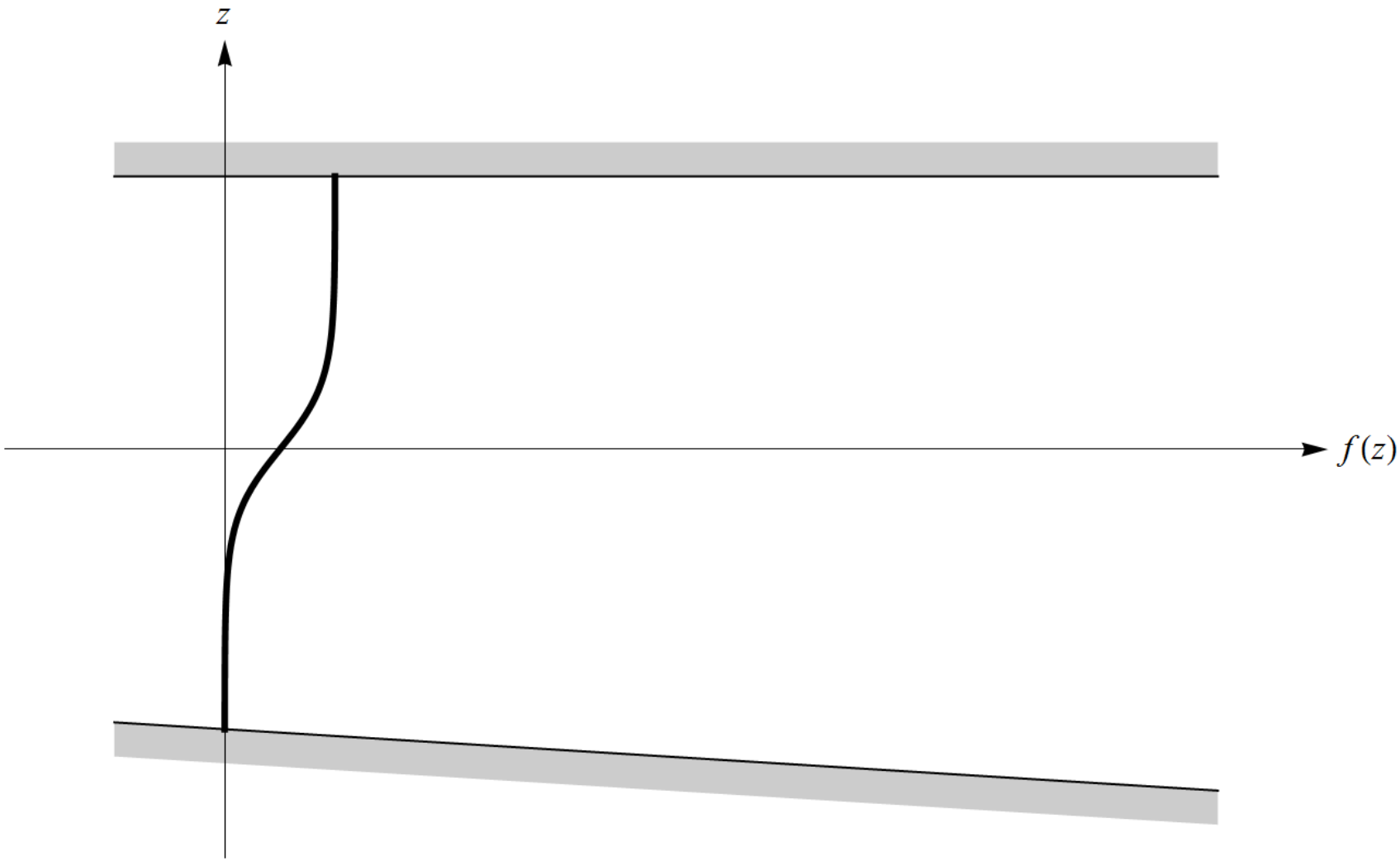

Sloping bottom boundary

- Topography variation of the sea bed may result in a finite range where AI will be present. Creating zone of AI parallel to the shore.

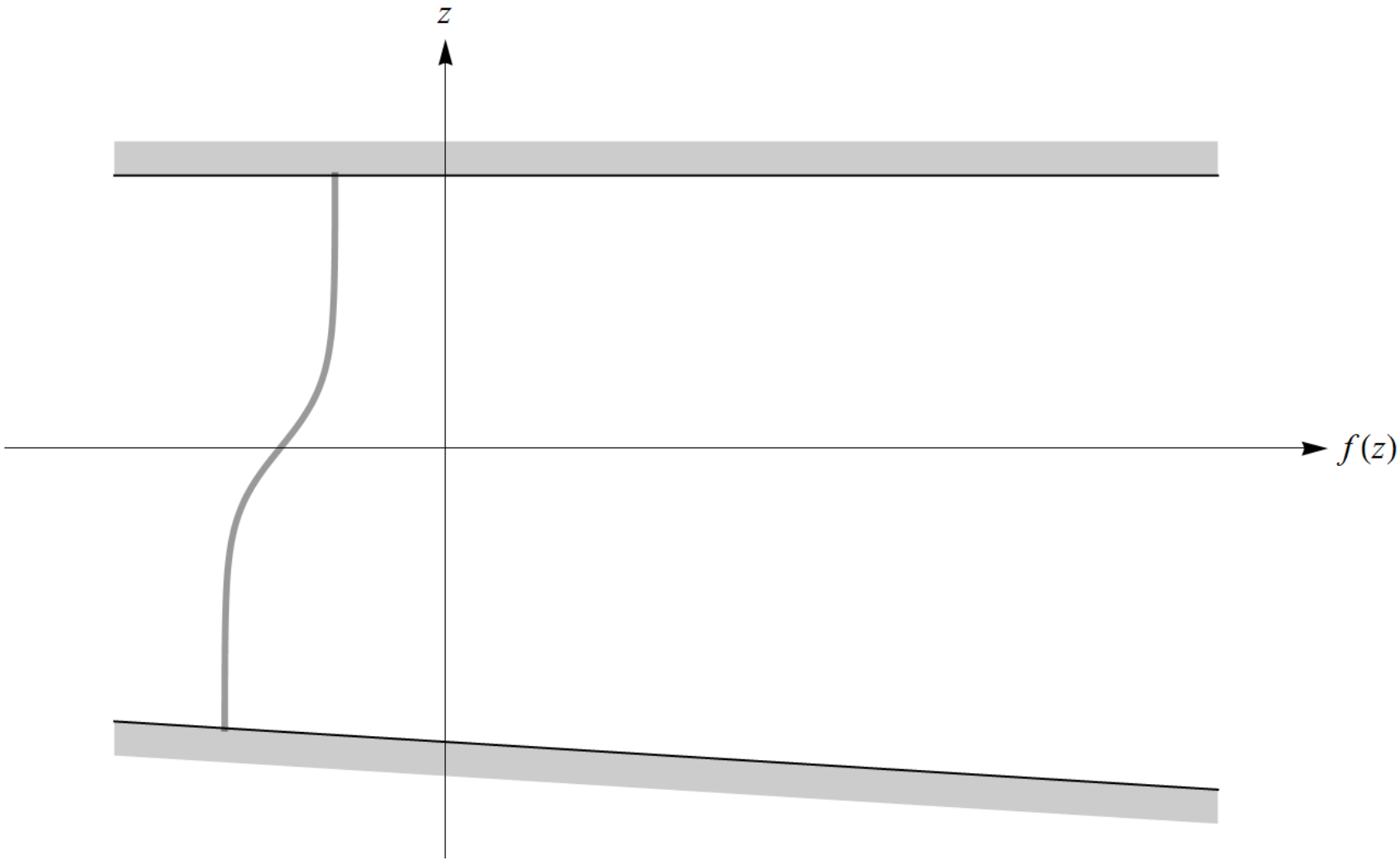

Sloping bottom boundary

- Topography variation of the sea bed may result in a finite range where AI will be present. Creating zone of AI parallel to the shore.

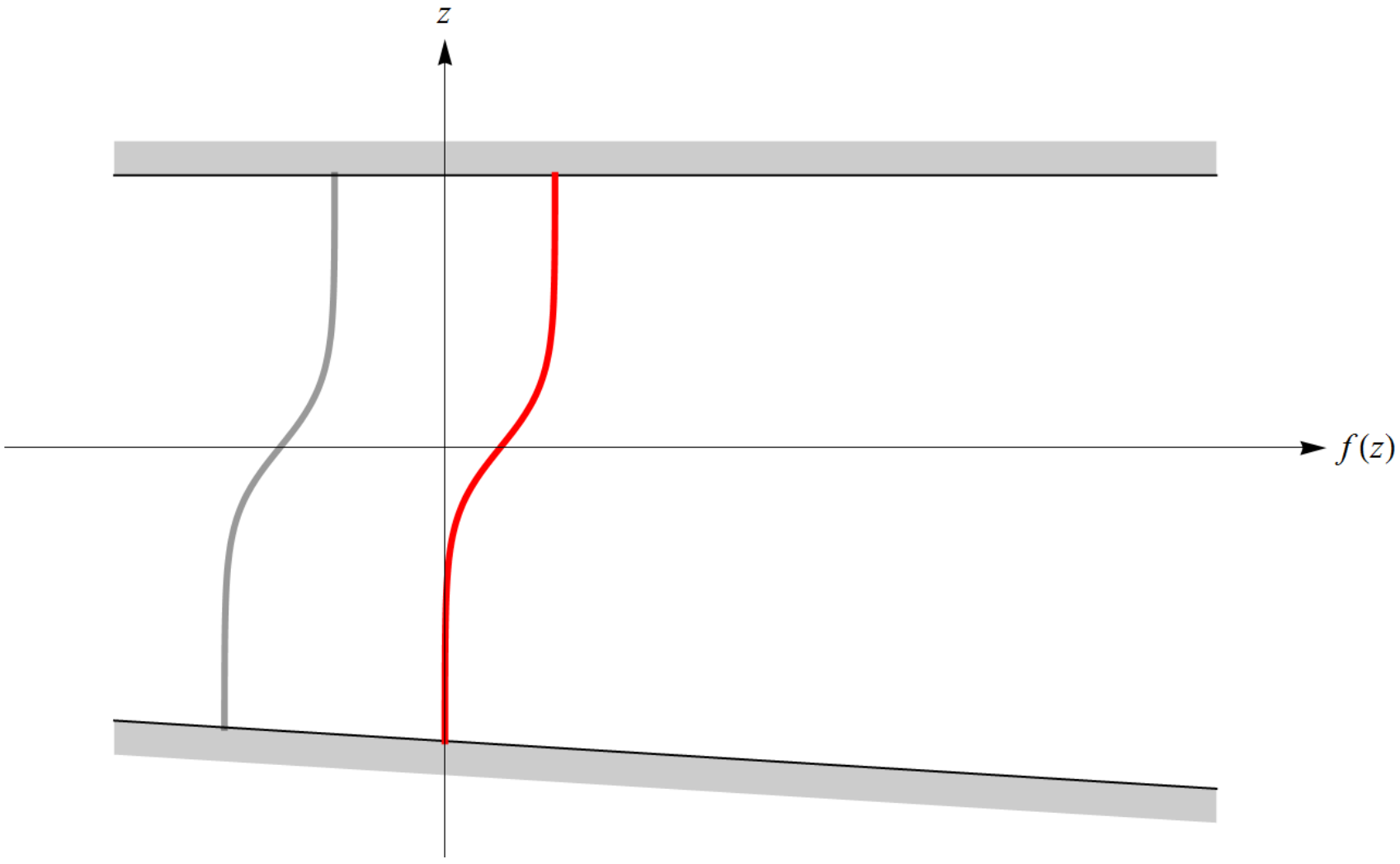

Sloping bottom boundary

- Topography variation of the sea bed may result in a finite range where AI will be present. Creating zone of AI parallel to the shore.

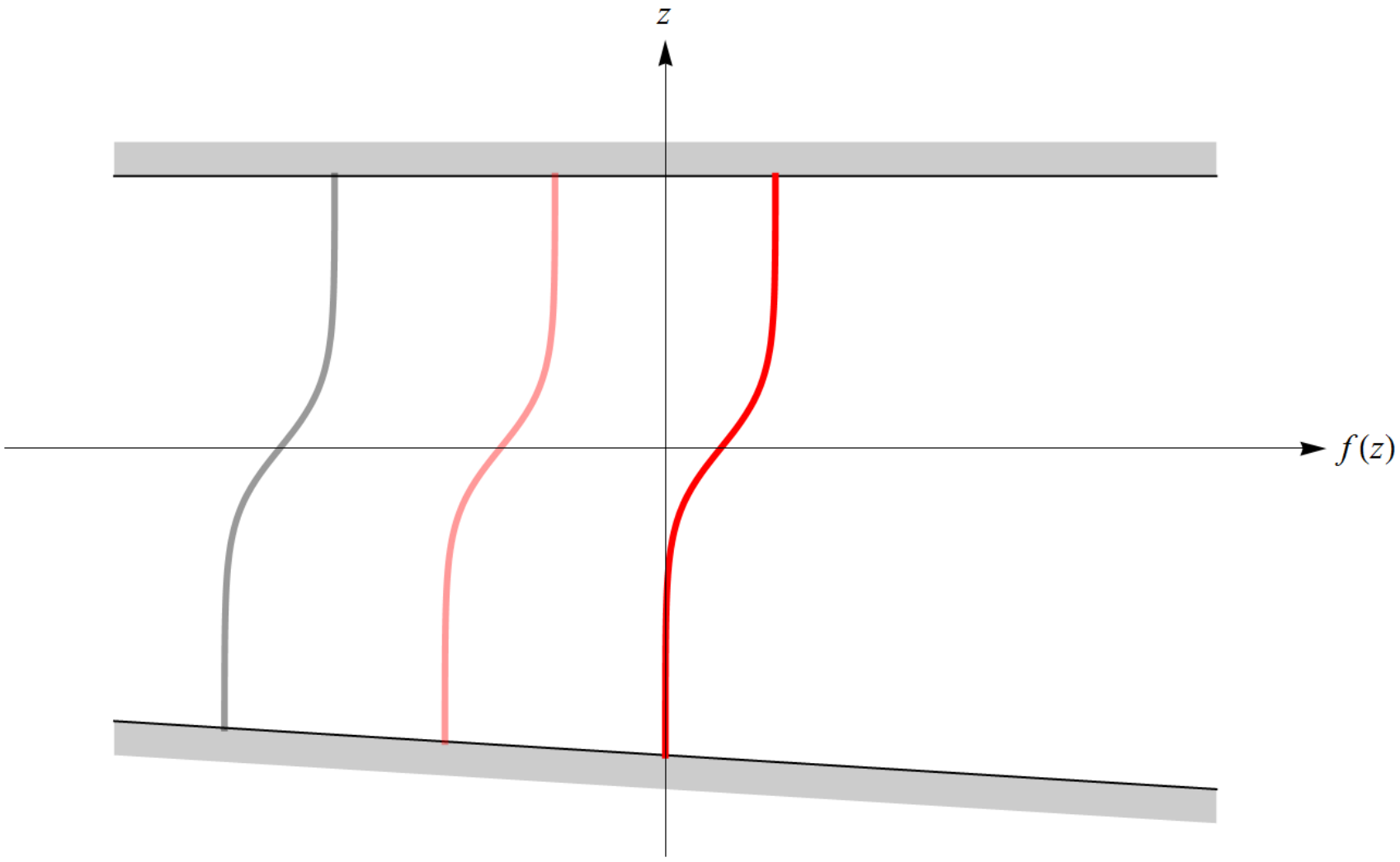

Sloping bottom boundary

- Topography variation of the sea bed may result in a finite range where AI will be present. Creating zone of AI parallel to the shore.

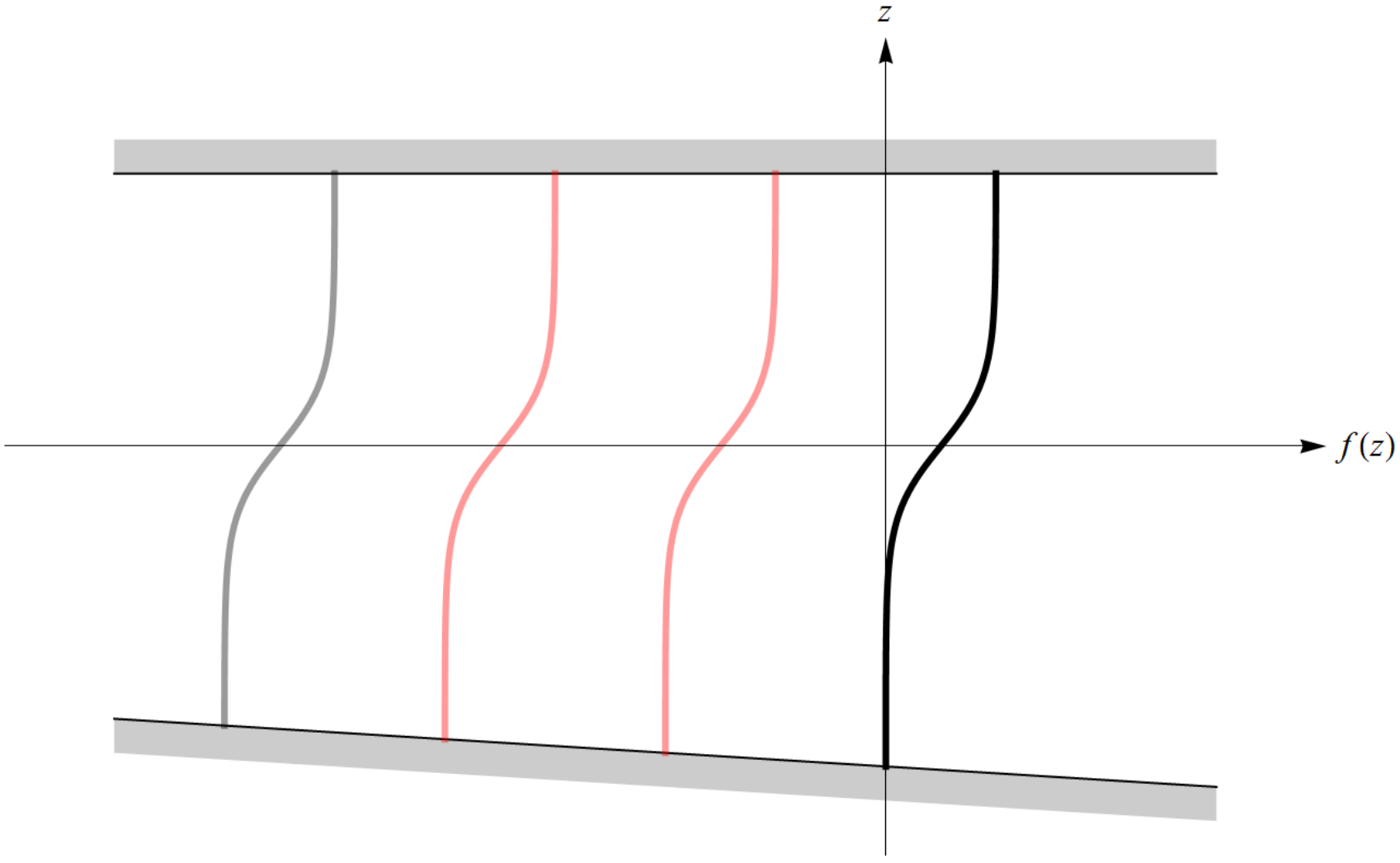

Sloping bottom boundary

- Topography variation of the sea bed may result in a finite range where AI will be present. Creating zone of AI parallel to the shore.

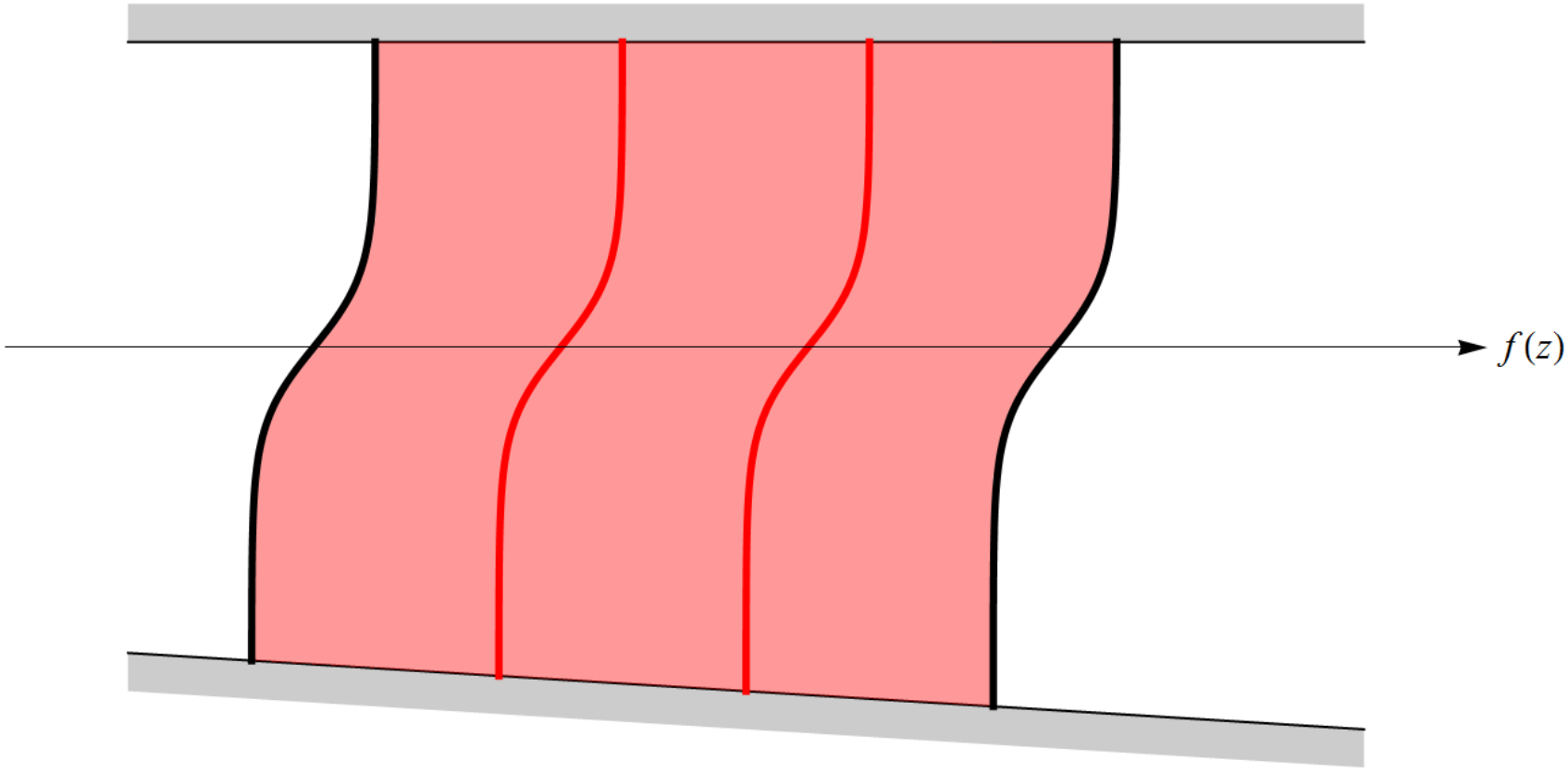

Globally unstable?

- The variation of the bottom boundary in the region where AI is present can be considered as a slow spatial variation of the whole flow and mainly its complex dispersion relation $\omega(\alpha_i, \alpha_r)$.
- At leading order the global mode frequency at the saddle point where $\frac{\partial \omega}{\partial \alpha} = 0$ and $\frac{\partial \omega}{\partial X} = 0$ (see Soward and Jones 1983),

$$\omega_G = \omega_0(X_s) \tag{6}$$

where X is the new spatial variable.

Spatially varying bottom boundary

- We define the distance of bottom boundary $h_2(X) = r_c(X)h_1$.
- Note that if the problem is parallel then $\frac{\partial \omega}{\partial X} = 0$ and the resultant absolutely unstable flow will be also globally unstable.
- We consider first linearly varying bottom boundary by letting

$$r_c(X) = X + 2.5, \tag{7}$$

and let $h_1 = 10$ say.

Linearly varying bottom boundary

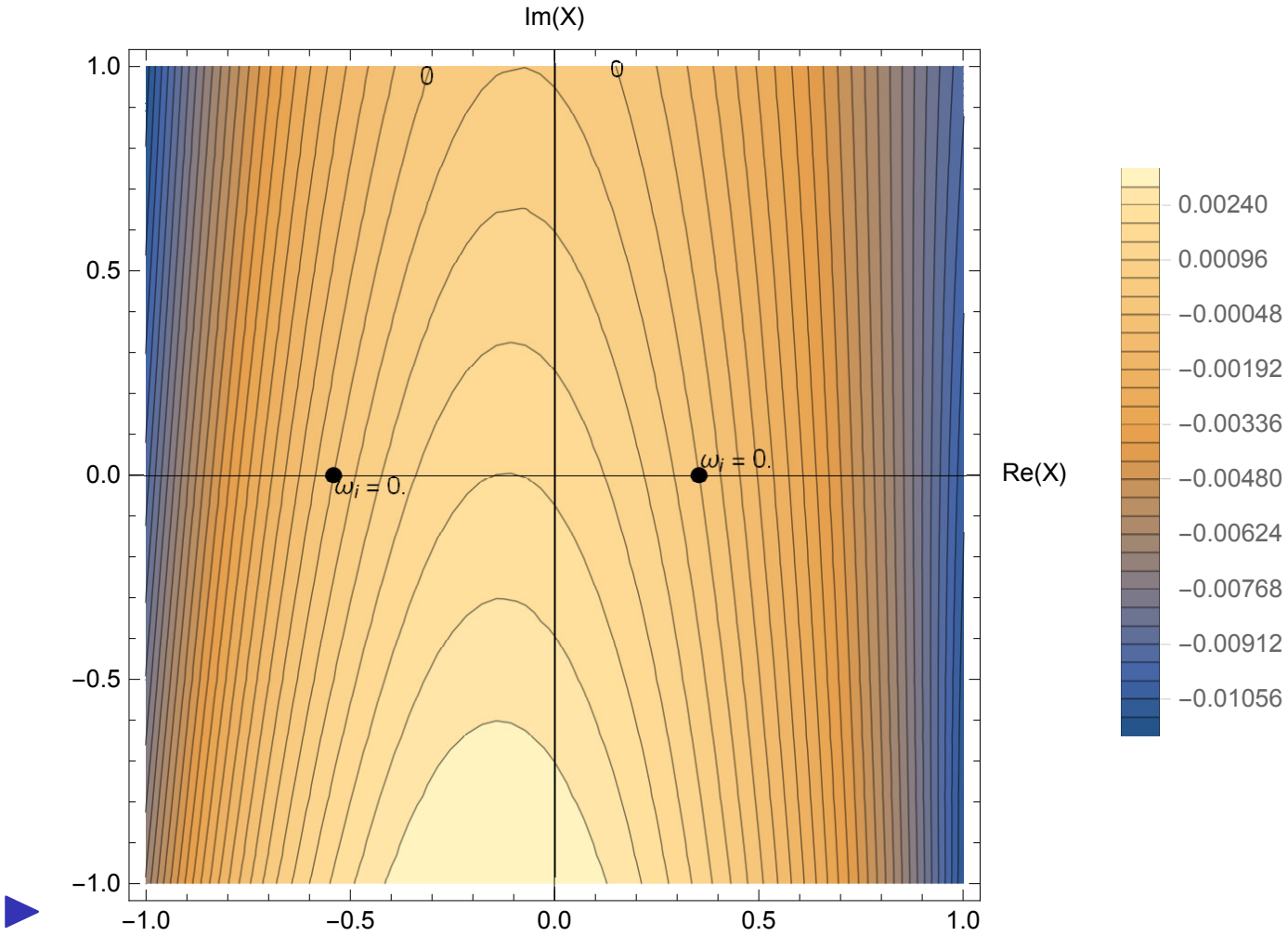

- Contours of constant $\mathrm{Im}(\omega)$ at pinch points in the complex $X-$plane for linearly varying bottom boundary with upper boundary placed at $h_1 = 10$. The solid discs are intersection of the zero contour with the real axis at -0.54 and 0.35.

Bottom boundary with maxima and minima

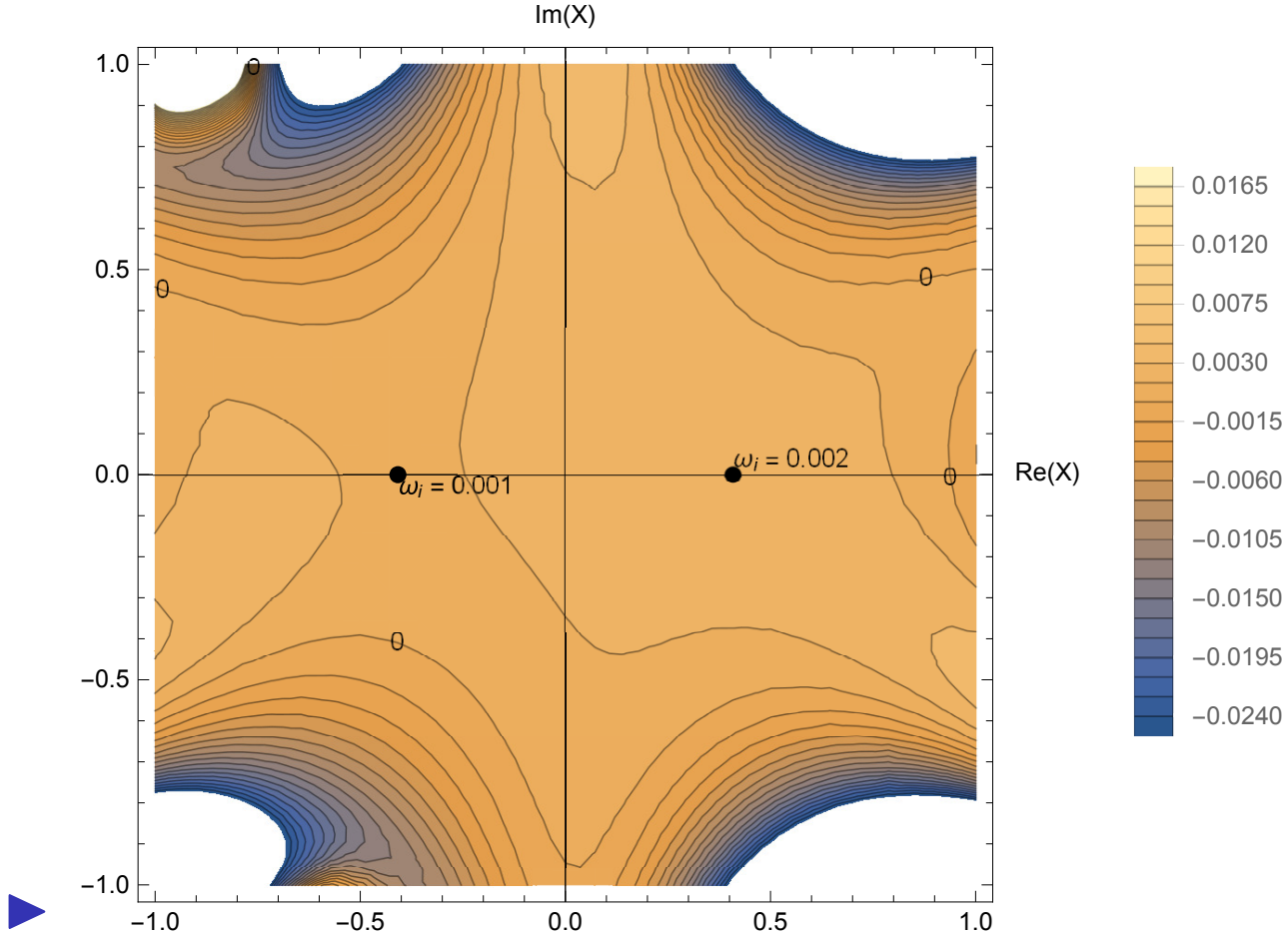

- $r_c(X) = X^3 - 0.5X + 2.5$. Contours of constant $\mathrm{Im}(\omega)$ at pinch points in the complex $X-$plane for bottom boundary with maxima and minima, and upper boundary placed at $h_1 = 10$. The solid discs are the double saddle points satisfying $\frac{\partial \omega}{\partial \alpha} = 0$ and $\frac{\partial \omega}{\partial X} = 0$ at $X = \pm(0.5/3)^{1/2}$.

Monotonically increasing bottom boundary

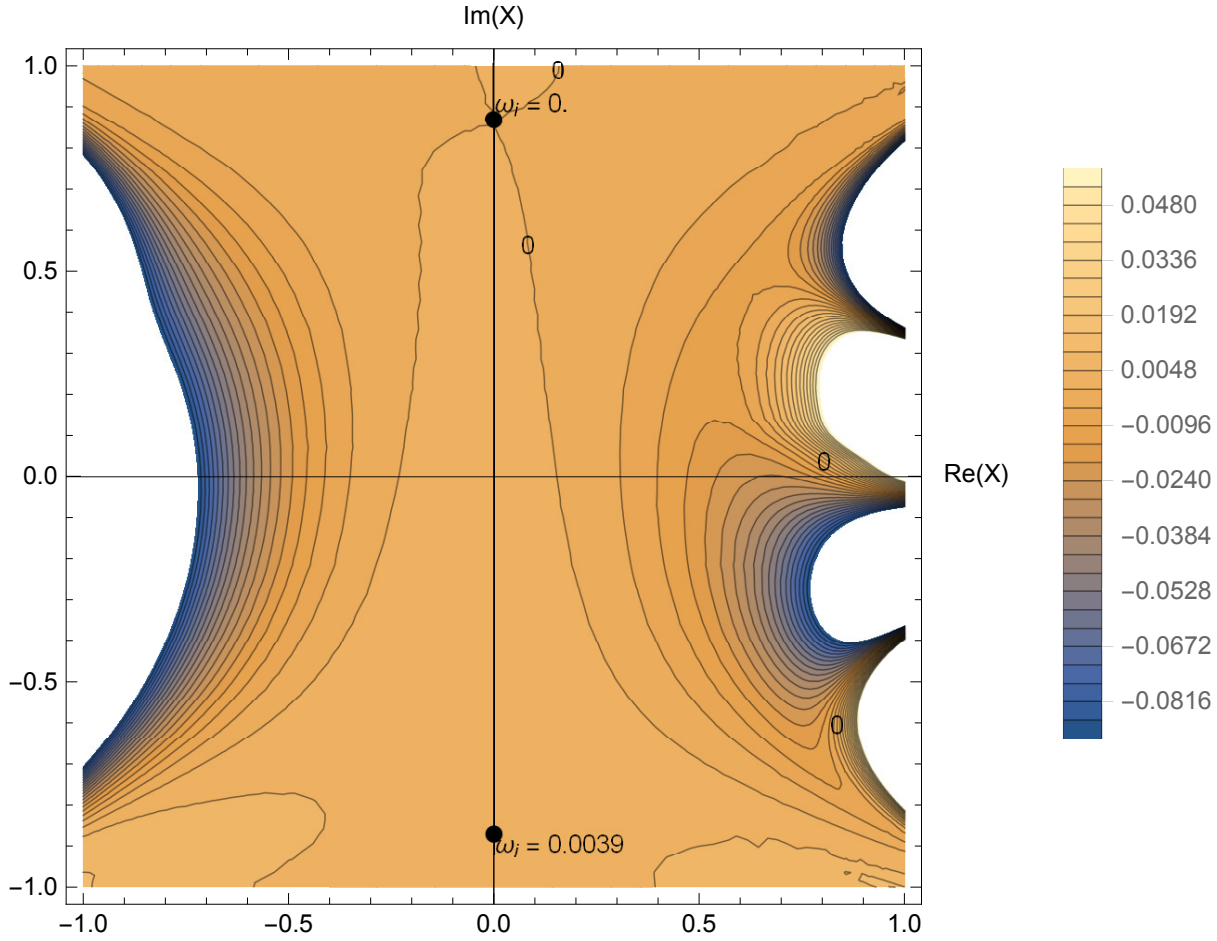

- $r_c(X) = X^3 + 2.27X + 2.5$. Contours of constant $\mathrm{Im}(\omega)$ at pinch points in the complex $X-$plane for monotonic boundary, and upper boundary placed at $h_1 = 10$. The solid discs are the double saddle points satisfying $\frac{\partial \omega}{\partial \alpha} = 0$ and $\frac{\partial \omega}{\partial X} = 0$.

Conclusion

- We present the parameter space for AI to occur in a co-flow problem with two boundaries. Maximum for $J_0 \approx 0.025$ with boundaries placed at particular position $h_1 \approx 1, r_c \approx 2.5$
- We present model results of global stability analysis for spatially varying bottom boundary typical in near shore sea regions, and show that there is a possibility of global instability for monotonically decreasing (or increasing) sea bed.

References

- P. Huerre and P. Monkewitz, "Absolute and convective instabilities in free shear layers," *J. Fluid Mech.*, vol. 159, pp. 151–168, 1985.
- J. Healey, "Destabilizing effects of confinement on homogeneous mixing layers," *J. Fluid Mech.*, vol. 623, pp. 241–271, 2009.
- P. Drazin and W. Reid, *Hydrodynamic stability*. Cambridge University Press, 1981.
- R. Briggs, *Electron-Stream Interaction with Plasmas*. MIT Press, 1964.
- R. Danyi, "Global Instability of Mixing Layers Created by Confinement.," *PhD Thesis.*, Keele University, 2018.

Briggs saddle point method

- Consider localized unsteady forcing to undisturbed flow

$$\hat{v}(x, 0, t) = \delta(x)\hat{f}(t), \tag{8}$$

which is switched on at $t = 0$, where $\hat{f} = 0$ for $t < 0$. The response can be expressed in terms of double integral of normal modes over all wavenumbers and frequencies, which is obtained, from inverse Fourier transforms as

$$\hat{v}(x, y, t) = \frac{1}{4\pi^2} \int_F \int_A \frac{f(\omega)}{\Delta(\alpha, \omega)} v(y) e^{i(\alpha x - \omega t)} d\alpha d\omega, \tag{9}$$

where $\Delta = 0$ is the dispersion relation. Δ appears in the denominator and roots of $\Delta = 0$ give non-trivial solutions when the forcing is switched off. Integration contours F and A run from $-\infty$ to $+\infty$, but not necessarily along the real axes. Roots of the dispersion relation $\Delta = 0$ produce poles in (9).

Briggs saddle point method

Placing F contour above all poles ensure causalities (no response for $t < 0$). If we can lower the F or A contour onto the real axes, then this corresponds to spatial or temporal stability analysis.

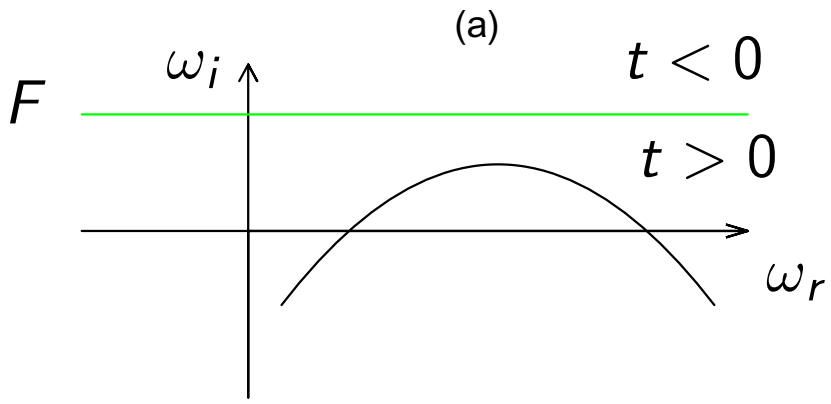

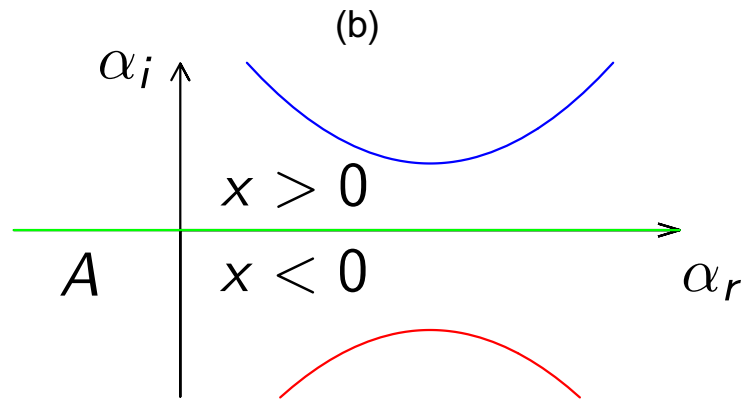

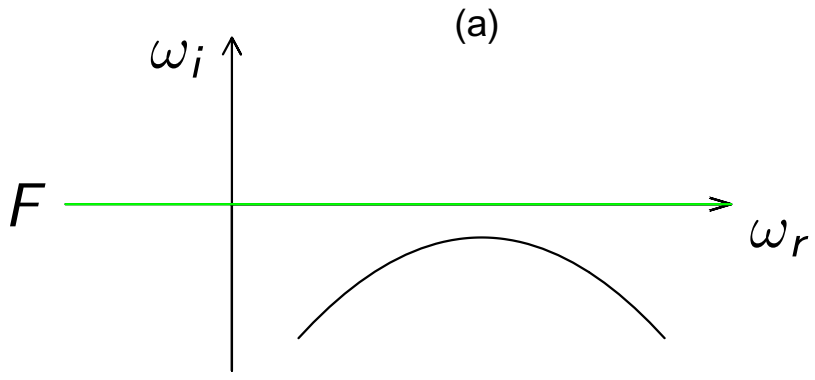

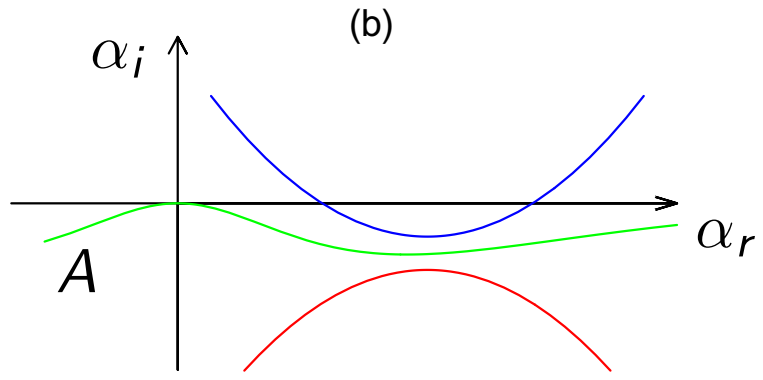

Briggs saddle point method

Sometimes F can not be lowered to the real ω-axis

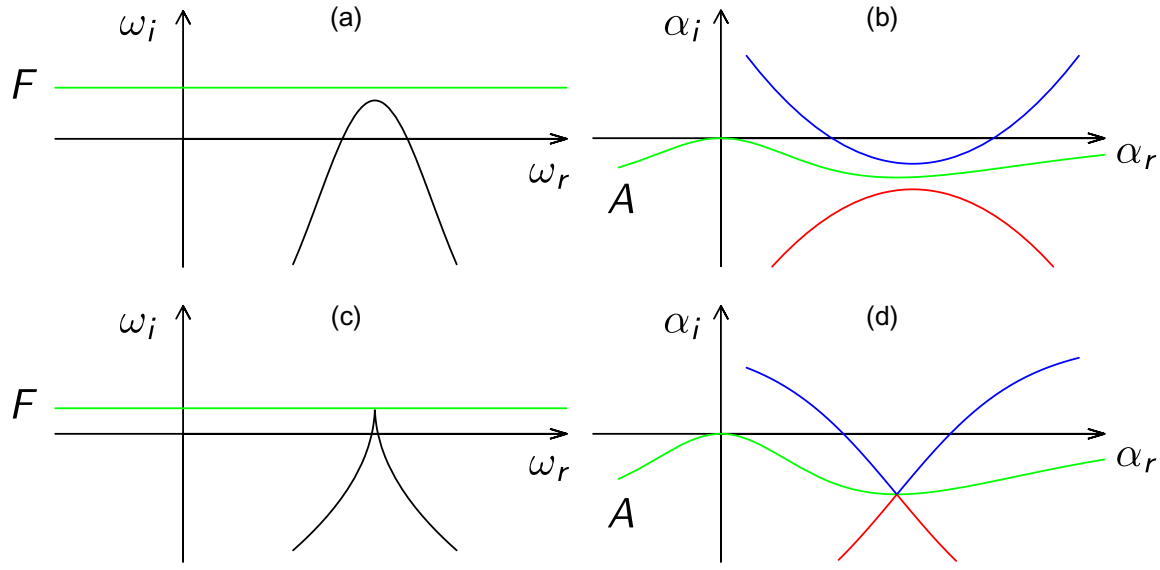

Resultant dispersion relation, black line, in complex ω-plane shown in part (a) and (c) with the placement of integration contour F. In part (b) and (d)is the dispersion relation in the complex α-plane, blue and red lines (which corresponds to downstream and upstream propagating waves).The A contour is then said to be pinched by spatial branches as shown in figure 26 (d), Im(ω) at the pinch point gives the growth rate in time of the absolute instability.

Briggs saddle point method

The difference in physical behaviour of convectively unstable flow and absolutely unstable flow can be found from considering the response to an impulsive disturbance. Therefore we consider an impulsive disturbance, $f(\omega) = 1$, and use the residue theorem to evaluate the ω-integral in (9) first. This leaves the α-integral in the form

$$\hat{v} = \int_A -\frac{2\pi i}{\Delta_\omega} v(y) e^{i(\alpha x - \omega(\alpha) t)} d\alpha = \int_A -\frac{2\pi i}{\Delta_\omega} v(y) e^{\phi t} d\alpha, \quad (10)$$

where

$$\phi(\alpha) = i(\alpha \frac{x}{t} - \omega(\alpha)). \quad (11)$$

Briggs saddle point method

$\omega(\alpha)$ in (11) is a root of $\Delta = 0$ since the roots of $\Delta = 0$ gives poles captured by the residue theorem. This is a superposition of normal modes satisfying the dispersion relation, where the factor Δ_ω represents the receptivity to disturbances of different frequencies. In the limit $t \to \infty$ the integral (11) is dominated by the contribution from the saddle-point at which

$$\frac{d\phi}{d\alpha} = 0 \implies \frac{d\omega}{d\alpha} = \frac{x}{t}. \tag{12}$$

This is because away from the saddles the integrand in (11) is highly oscillatory, leading to substantial cancellation. At the saddle the phase of ϕ is stationary and hence the integrand is non-oscillatory near the saddle. We locate the saddle points of ϕ by plotting contours of constant Re(ϕ) in the complex-α plane, as shown in the next figure.

Briggs saddle point method

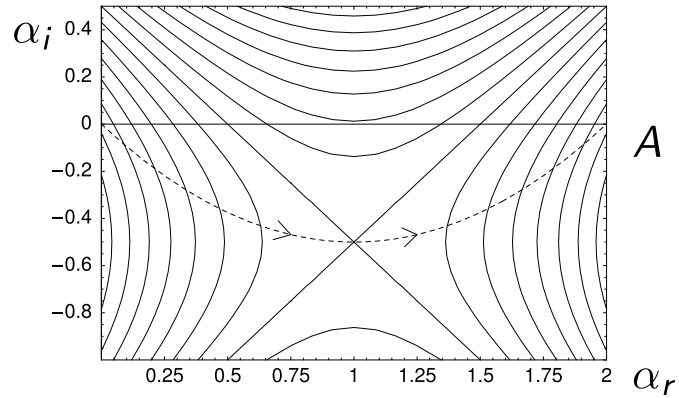

Figure: Deformation of A contour, dashed line, in the complex α-plane passing through the saddle point.

The saddles that contribute to the solution are those that have valleys along the real wavenumber axis. The A integration contour through such a saddle then follows a steepest descent path from the saddle point. The large-t behaviour in different frames of reference is found by choosing different values of x/t in (12). In the rest frame the large-t behaviour is given by

$$\frac{x}{t} = 0, \text{ and hence } \frac{\partial \omega}{\partial \alpha} = 0. \tag{13}$$

Briggs saddle point method

which corresponds to zero group velocity. When $x/t = 0, \phi = -\mathrm{i}\omega$, so contours of $\mathrm{Re}(\phi)$ are equal to contours of $\mathrm{Im}(\omega)$, which corresponds to roots of the dispersion relation $\Delta = 0$ for horizontal F-integration contours, i.e. spatial branches in the complex α-plane. Therefore, locating saddles and steepest-descent valleys corresponds to finding the spatial branches that pinch the integration contours in Brigg's method.
The condition for absolute instability, i.e. for growth in the rest frame, is therefore

$$\frac{\partial \omega}{\partial \alpha} = 0, \mathrm{Im}(\omega) > 0. \tag{14}$$

Global instability

WKB theory provides the framework for studying waves in slowly varying flows, and local dispersion relations appear at leading order. The normal mode form for disturbances appropriate to parallel flow is replaced by a product of an envelope function that varies in the streamwise direction on the slow scale of the basic flow, and an exponential term that varies on the fast scale of the disturbance wavelength.

$$A(X)v(X,y)\exp i\left(\int \alpha(X)dX - \omega t\right). \qquad (15)$$

The envelope function usually satisfies a first order differential equation, whose solution describes the slow variation in the amplitude of the wave in the streamwise direction due to non-parallel effects (there is also a faster amplitude dependence associated with the exponential term, which is determined by local dispersion relations) $\partial\omega_0/\partial\alpha A' + \{...\}A = 0$.

Global instability

However 'turning points' in WKB theory can exist, which are values of the streamwise coordinate, $X = X_t$, where the envelope evolves on a faster scale, and where several modes interact. In such situation near X_t, A might satisfy $A'' - (X - X_t)A = 0$, allowing both upstream and downstream boundary conditions to be satisfied. A global mode has a turning point at X_t, where $\omega_G = \omega_0(X_t)$ and ω_0 is the local absolute frequency satysfying $\partial\omega_0/\partial\alpha = 0$.

Global instability

For example if $\omega_0 = constant = \omega_G$,

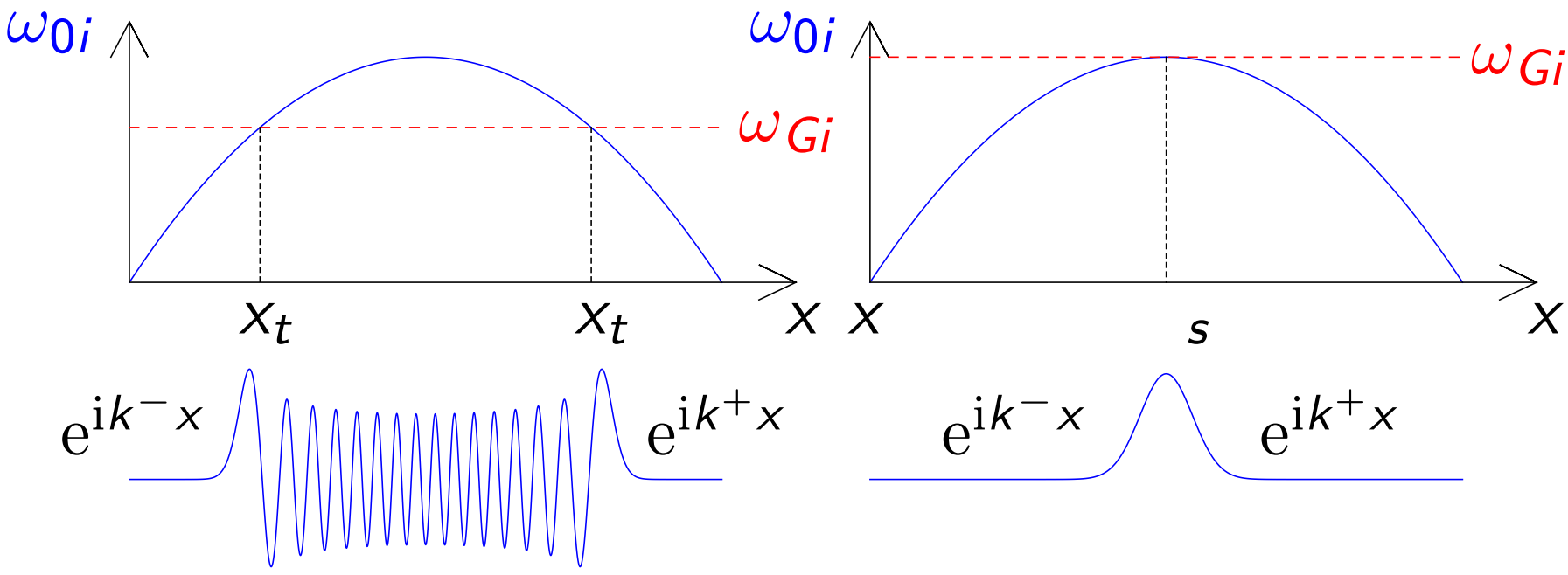

The most unstable global mode satisfies the saddle condition $\partial\omega_0/\partial X = 0$. In particular, for envelopes that decay to zero as $X \to \pm\infty$, it was shown by Soward and Jones (1983) that the most unstable (or least damped) global mode corresponds to the double saddle condition $\frac{\partial\omega}{\partial\alpha} = 0, \frac{\partial\omega}{\partial X} = 0$.